J. Eng. Sci., Univ. Riyadh, Vol. 7 (1), pp. 43 - 51 (1981)

Synchronous Machines Performance in HVDC Networks as Affected by Saliency & Controlled and Uncontrolled Commutation

M.A.Shimy Mansour*, Abdulaziz A.El-Sulaiman and S.Abdelrahzak*****

* *(Late) Professor of Electrical Engineering, College of Engineering, University, of Riyadh;*

** *Assistant Professor of Electrical Engineering, College of Engineering, University of Riyadh;*

*** *Faculty of Engineering, Cairo University, Egypt.*

Theoretical and experimental characteristics of a synchronous machine are developed for HVDC networks with rigorous account for saliency and commutation(uncontrolled and controlled operation). The system performance equations are represented with and without damper circuits. The treatment given by this paper can be adapted to sepcial cases such as turbo-type machines. A comparative study is provided by comparing the computer results with the actual test results.

Nomenclature

α	Bridge delay angle
γ	Commutation angle
δ	Displacement angle
β	Interval variable
R_e	Thyristor resistance
L_e	Thyristor inductance
i_a, i_b, i_c	Armature phase current
I_e	Load current
V_e	Output voltage
V_a, V_b, v_c	Armature phase voltage
i_f	Field current
i_h, i_g	Damper currents
ψ_i	Flux-linkage of circuit i
L_d	Direct-axis synchronous inductance
L_q	Quadrature-axis synchronous inductance
L''_d	Direct-axis subtransient inductance
L''_q	Quadrature-axis subtransient inductance
L_{ij}	Inductance between rotor circuit i and j.
$(i_f)_\gamma$	Field current at the end of commutation period
$(i_g)_\gamma\ (i_h)_\gamma$	Damper current at the end of commutation period
$(i_f)_o$	Field current at the beginning of commutation period
$(i_g)_o\ (i_h)_o$	Damper current at the beginning of commutation period
W & H	Integral functions.

1. Introduction

A basic paper by Gerecke [1] extended the classical theory of synchronous machines working with controlled values on D.C.load. Garrido [2] gave a study of steady state and transient analysis of generator-rectifier circuit. A similar approach was outlined in another paper by Bugenstein [3] which explained the very high transients phenomenon observed during the application and removal of load. Franklin [4] gave theoretical equations describing the relation between the performance and design of three phase salient pole type generator with simultaneous AC and DC output, the solution of the basic set of equations required an iteration process, which can, however, be replaced by sufficiently accurate equations derived by the use of two simple assumptions. Bonwick [5] investigated the theoretical and experimental performance of synchronous generator connected to controlled and uncontrolled bridge rectifier loads. The performance equations have been derived for a cylindrical rotor generator with symmetrical damper windings based on the assumption of constant flux linkages.

This paper is an extension of the studies carried out by Bonwick and Franklin and is concerned with solving some problems related to the field and damper currents. In additon, the performance of salient pole synchronous generator, with and without asymmetrical damper windings, which is connected to controlled bridge rectifier load was investigated.

Experimental results for the several cases were in agreement with the digital computation results. Oscillogram records at the transients during operating with the load variation at different controlled delay angle, for AC phase voltage, field current, and DC output voltage were recorded.

2. Performance of a Salient Pole Type Generator with Damper Windings Connected to Controlled and Uncontrolled Bridge Rectifier for Overlap Angle Equal to $\pi/3$

Circuit Description

In this paper, a 4-pole 3-phase salient pole type generator with asymmetrical winding is considered. The generator is loaded by a 6-element thyristor bridge which has a resistance R_e in series with an infinite inductance L_e connected to its D.C. load terminals.

Fig.(1) shows the well known relations between phase voltage and currents for an overlap $\gamma < 60°$ and zero delay. It is now to be noted that within each basic cycle of 360° equal subcycles of 60° exist (Section AB) of Fig.(2). Fig (3) shows the relation between phase voltage and current for an overlap angle $\gamma < 60°$ and with controlled bridge delay angle (α).

The case of over-lap angle equal to $\pi/3$ is very important specially at short circuit condition or pure

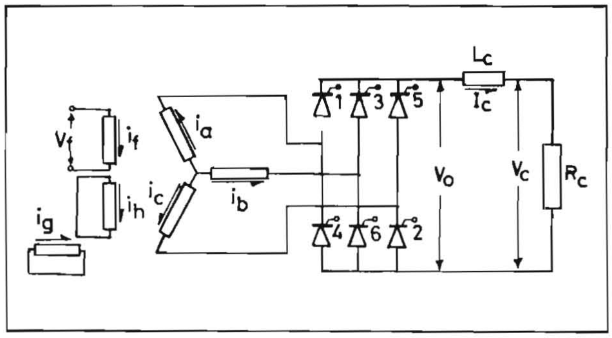

Fig. 1. The synchronous generator with direct and quadrature axis damper winding with bridge load.

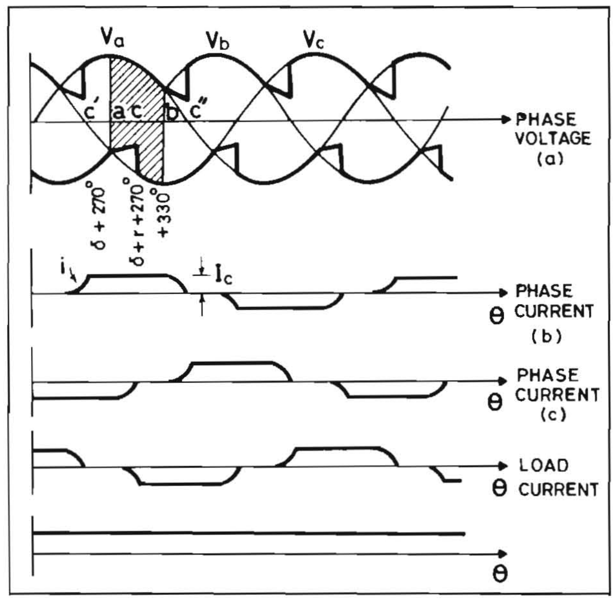

Fig. 2. Voltage and current relations for star connected armature windings (60°) with delay angle = 0

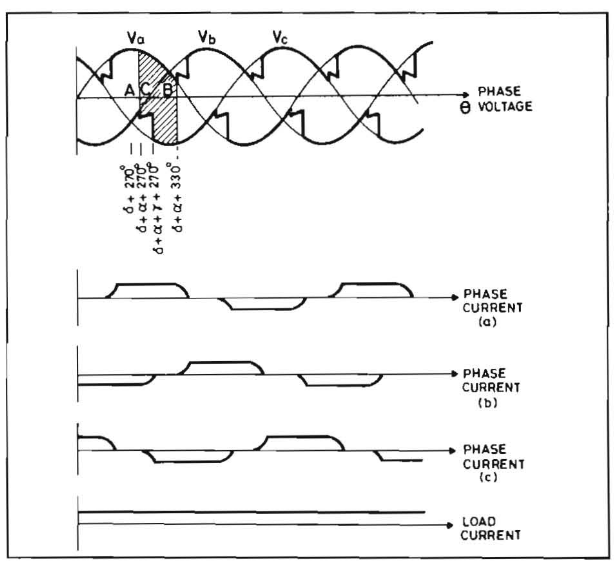

Fig. 3. Voltage and current relations for star connected armature windings (60°) with a delay angle .

inductive loading. In this case phases (b)and(c)are to commute for the full duration of the subcycle AB and the interlude intervals between commutation is zero.

2.1 Field and Damper Current Equations

The field and damper currents can be written in the following form, bearing in mind that it has been substituted for $\gamma = \pi/3$; then

$$i_f = I_f + \sqrt{3}\, K_f I_e\, [\sin(\delta + \alpha + \beta + 30) - \sin(\delta + \alpha + \beta + 30)] - \sqrt{3} K_f\, i \cos(\delta + \alpha + \beta) \quad (2.1)$$

$$i_h = (i_f - I_f) K_h / k_f \quad (2.2)$$

$$i_g = 0 + \sqrt{3}\, K_g I_e\, [\cos(\delta + \alpha + \beta + 30) - \cos(\delta + \alpha + 30)] + \sqrt{3}\, K_g\, i \sin(\delta + \alpha + \beta). \quad (2.3)$$

where K_f, K_h and K_g are defined in Appendix A.

It is clear from equation (2.1), (2.2) and (2.3) that the field current and damper currents are functions of bridge load current, displacement angle, transient commutation loop current, and synchronous machine parameters.

2.2 Deformation of the Voltage Wave-form due to Commutation

With substituting for $\gamma = \pi/3$ into the instantaneous armature voltage equations

$$V_a = (2/\sqrt{3}\,W)\, I_e\, [(L''_q - L''_d) - (L_d - L_q)] \cos 2(\delta + \alpha + \beta - 30) - (2/\sqrt{3})\, W\, i[(L''_q - L''_d) - (L_d - L_q)] \cos 2(\delta + \alpha + \beta) - (1/\sqrt{3})(P\, i)\, [(L''_q - L''_d) - (L_d - L_q)] \sin 2(\delta + \alpha + \beta) + W L_f I_f \cos(\delta + \alpha + \beta) - (2/\sqrt{3}) \frac{W I_e \cos(\delta + \alpha + \beta)\, [L''_q - L''_d]\, (\cos(\delta + \alpha + \gamma - 30)}{(\pi/3) - \gamma}$$

$$- \cos(\gamma + \alpha + 30)] - (2/\sqrt{3}) \frac{W I_e \sin(\delta + \alpha + \beta)}{(\pi/3) - \gamma} [L_d - L_q][\sin(\delta + \alpha + \gamma - 30) - \sin(\delta + \alpha + \gamma + 30)]. \quad (2.4)$$

L''_q and L''_d are defined in Appendix A, whereas W & H are defined in Appendix B.

Same for V_b and V_c. Note that equation (2.4) can be easily adapted to cylindrical type. It can be simpler for the case of zero sub-transient saliency.

2.3 Displacement Angle Equation

The displacement angle equation with the new values of $(i_f)_o$, and for $\gamma = \pi/3$ can be written as follows:

$$(L_d - L_q) \sin 2(\delta + 60) = (L''_d - L''_q) K_1 \sin^2(\delta) + K_2 \sin(2\delta) + A(L_d - L''_q) + (\sqrt{3}/2 (L_d - L''_d) - \frac{\sqrt{3}\, I_e}{2 I_f} L_f \sin(\delta) \quad (2.5)$$

From equation (2.5), the displacement angle will be a constant value for a constant ratio of I_f / I_e. The constants K_1, K_2, A and B are defined in Appendix A.

2.4 Average D.C. Output Voltage

Substituting for the value of $\gamma = \pi/3$, we get

$$V_e = 9W/2\pi[I_e/\sqrt{3}(L_d - L_q) \sin 2(\delta + \alpha + 30) - L_f I_f \sin(\delta + \alpha - 60)] \quad (2.6)$$

For a constant excitation, and constant speed, the D.C.voltage will be a function of load current only, equation (2.6) represents the external characteristics of the system. It looks like the external characteristics of a rectifier loaded synchronous generator with damper windings at commutation angle equal to $\pi/3$. The average voltage for special cases such as cylindrical type synchronous generator, and uncontrolled loads, can be predicted.

3. Performance of Salient Pole Type Synchronous Generator with Damper Windings Connected to Controlled Bridge Rectifier Load

3.1 Performance Equations During Commutation Interval

For a given delay angle, commutation from phase b to phase c will commence at $\theta = (\delta + \alpha + \beta + 270)$. During commutation, the rotor angle $\theta_r = (\delta + \alpha + \beta + 270)$. ($\beta$ is the interval variable). The current matrix is then a column matrix shown for a star connection.

$$I = [I_e \; -I_e \; i \; -i \; i_f \; i_h \; i_g]^T \quad (3.1)$$

Also the voltage matrix is a column matrix,

$$V = [V_a \; V_b \; V_c \; V_f \; V_h \; V_g]^T = \frac{d\psi}{dt} = \omega \frac{d\psi}{d\theta} \quad (3.2)$$

The derivation of the basic equations start with the commutation equation.

$$V_b - V_c = w \frac{d}{d\theta}(\psi_b - \psi_c) = 0$$

From the commutation voltage constraint

$$\therefore \quad \psi_b - \psi_c = C \text{ (constant)} \qquad (3.3)$$

This can be written also to describe the commutation interval.

$$\psi_b - \psi_c = (L_{sa} + L_{ma}) I_e + 3L_{sv} I_e \cos(\delta + \alpha + \beta - 30)$$
$$-2(L_{sa}+L_{ma}) i - 3L_{sv} i \cos 2(\delta + \alpha + \beta)$$
$$-\sqrt{3}[L_f i_f + L_h i_h] \cos(\delta + \alpha + \beta)$$
$$+ 3[L_g i_g] \sin(\delta + \alpha + \beta) = C \qquad (3.4)$$

In order to calculate C, using a special limit *i. e.* begining of commutation load,

$\beta = 0$, $i_f = (i_f)_o$, $i_h = (i_h)_o$ $i = o$ and, $i_g = (i_g)_o$

and substituting in equation (3.3) for C to get equation (3.4) which involves the load current, displacement angle, transient commutation current, field current damper currents, and the machine parameters.

3.1.1 Field and damper current equations

Since the duration of the commutation event is usually small compared with the circuit time constants, then constant flux linkages exist in the field and damper magnetic circuit is assumed. A useful relationship for field and damper magnetic circuit is assumed. A useful relationship for field and damper currents can be readily determined. Therefore, the flux linkage equations during commutation become:

$$\psi_f = -\sqrt{3}L_f I_e \sin(\delta + \alpha + \beta + 30) + 3L_f i \cos(\delta + \alpha + \beta) + L_{ff} i_f + L_{fh} i_h$$

$$\psi_h = -\sqrt{3}L_h I_e \sin(\delta + \alpha + \beta + 30) + 3L_h i \cos(\delta + \alpha + \beta) + L_{HF} I_f + L_{hh} i_h$$

$$\psi_g = -\sqrt{3}L_g I_e \cos(\delta + \alpha + \beta + 30) - 3L_g i \sin(\delta + \alpha + \beta) + L_{gg} i_g \qquad (3.5)$$

applying the initial conditions stated earlier, equation (3.5) becomes:

$$i_f = (i_f)_o + 3K_f (I_e [\sin(\delta + \alpha + \beta + 30) - \sin(\delta + \alpha + 30)] - i \cos(\delta + \alpha + \beta))$$

$$i_h = (i_h)_o + 3K_h (I_e [\sin(\delta + \alpha + \beta + 30) - \sin(\delta + \alpha + 30)] - i \cos(\delta + \alpha + \beta))$$

$$i_g = (i_g)_o + 3K_g (I_e [\cos(\delta + \alpha + \beta + 30) - \cos(\delta + \alpha + 30)] + i \sin(\delta + \alpha + \beta)) \qquad (3.6)$$

It can be seen from equation (3.6) that the field current and damper currents are function of bridge load current, displacement angle, transient commutation loop current, and synchronous machine parameters.

3.1.2 Commutation Equation

By eliminating i_f, i_h and i_g from equation (3.6) above and substituting $\beta = 0$, $i = o$, $i_f = (i_f)_o$, $i_h = (i_h)_o$ and $i_g = (i_g)_o$ we get

$$0 = I_e[L''_d - L_d] (\sin(\delta + \alpha + 30) - \sin(\delta + \alpha + \beta + 30)] \cos(\delta + \alpha + \beta) - i[L''_d - [L_d - L_q + L''_d - L''_q] (\delta + \alpha + \beta)] - I_e [L_d - L''_q] (\cos(\delta + \alpha + 30) - \cos(\delta + \alpha + \beta + 30)] \sin(\delta + \alpha + \beta) - (3/2)[L_f (i_f)_o + L_h (i_h)_o] [\cos(\delta + \alpha + \beta) - \cos(\delta + \alpha) + (3/2)[L_g (i_g)_o] [\sin(\delta + \alpha + \beta) - \sin(\delta + \alpha)] + I_e[L_d - L_q] [\cos^2(\delta + \alpha + \beta - 30) - \cos^2(\delta + \alpha - 30)]. \quad (3.7)$$

This gives the bridge-load current in terms of transient commutation current, displacement angle, and machine parameters. The commutation angle can be found by substitutuing $i = I_e$ and $\beta = \gamma$ in Equation (3.7).

3.1.3 Calculation of transient commutation current (i)

It will be remembered that the phase (b) and phase (c) are short circuited during commutation period and there is a transient commutation current flow from phase (b) to phase (c), this current at the end of cómmutation is equal to I_e and that can be found by rearrangement of equation (3.6).

3.2 Performance Equation During Interlude Interval between Commutation

Following the commutation interval, there will be an interlude between commutation of $(\pi/3) - \gamma$ During. the specific period under discussion, the current distribution can be written in a column matrix, this interval commences at $\beta = \gamma$, and the field and damper currents are $(i_f)_\gamma$, $(i_h)_\gamma$ and $(i_g)_\gamma$. By symmetry, the interlude interval ends at $\beta = 60°$ with the field and damper currents at their initial values $(i_f)_o$, $(i_h)_o$ and $(i_g)_o$. The current matrix during this interval is given by

$$I = [I_e \; - I_e \; i'_f \; i'_h \; i'_g]^T \qquad (3.8)$$

3.2.1 Field and Damper currents equations

A relationship for field and damper currents can be determined from the flux linkage, inductance equation, and equation (3.8). With the initial conditions stated above, the field equations can be written as follows:

$$\psi_f = -\sqrt{3} L_f I_e \sin(\delta+\alpha+\beta-30) + L_{ff}(i_f) + L_{fh}(i_h)$$

$$\psi_h = -\sqrt{3} L_h I_e \sin(\delta+\alpha+\beta-30) + L_{fh}(i_f) + L_{hh}(i_h)$$

$$\psi_g = -\sqrt{3} L_g I_e \cos(\delta+\alpha+\beta-30) + L_{gg}(i_g) \qquad (3.9)$$

The field current and damper currents for the interlude interval between commutations are obtained from equation (3.9) by assuming constant flux linkages.

$$i'_f = (i_f)_\gamma + 3K_f I_e [\sin(\delta+\alpha+\beta-30) - \sin(\delta+\alpha+\beta-30)]$$

$$i'_h = (i_h)_\gamma + 3K_h I_e [\sin(\delta+\alpha+\beta-30) - \sin(\delta+\alpha+\beta-30)]$$

$$i'_g = (i_g)_\gamma + 3K_g I_e [\cos(\delta+\alpha+\beta-30) - \cos(\delta+\alpha+\beta-30)] \qquad (3.10)$$

3.2.2 The field and damper current perturbation

Due to the operation of synchronous generator under rectified load, the field and damper current perturb from the begining to the end of commutation period. The field and damper current perturbation is found from current equations with $\beta = 60°$ and $i_f = (i_f)_o$ and that leads to conclude the field and damper current perturbation are directly proportional to the load current.

3.3 Deformation of the A V Voltage due to Commutation

Due to the overlap between phases (b) and (c) (two phase short circuit) the phase voltage waveforms are deformed, this deformation can be illustrated by phase voltages relationships. Substituting from the flux linkage equation, inductance equation, also substituting for i_f, i_h and i_g in order to get a relationship for each V_a, V_b and V_c; then we can get $(i_f)_o$, $(i_h)_o$ and $(i_g)_o$. The instantaneous value of armature voltages during commutation interval becomes

$$V_a = (2/\sqrt{3})\, W I_e [(L''_q - L''_d) - (L_d - L_q)] \cos 2(\delta+\alpha+\beta-30)$$

$$- (2/\sqrt{3})\, W i\, [L''_q - L''_d] - (L_d - L_q) \cos 2(\delta+\alpha+\beta)$$

$$- (1/\sqrt{3})(p\, i)[L''_q - L''_d] - (L_d - L_q) \sin 2(\delta+\alpha+\beta)$$

$$+ W L_f I_f \cos(\delta+\alpha+\beta) - (2/\sqrt{3}) \frac{W I_e \cos(\delta+\alpha+\beta)}{(\pi/3)-\gamma} [L_d - L''_d][\cos(\delta+\alpha+\beta-30)]$$

$$- \cos(\delta+\alpha+30) - (2/\sqrt{3}) \frac{W I_e \sin(\delta+\alpha+\beta)}{(\pi/3)-\gamma} [L_d - L''_d]$$

$$[\sin(\delta+\alpha+\gamma-30) - \sin(\delta+\alpha+\gamma+30))] \qquad (3.11)$$

Same for V_b and V_c.

Note that equation (3.11) can be easily adapted to cylindrical type. They can be simpler for the case of zero substransient saliency.

3.4 Displacement Equation

Displacement angle is the angular change in the intersection of line - to - neutral voltage waveforms, caused by the load current. It is measured as the angular difference between the point of intersection of two voltage waveforms on open circuit and their point of intersection on load.

The interlude armature voltages V_a and V_b are equal at $\beta = 60 - \alpha$ and this leads to the displacement equation. Then

$$V_b - V_c = 0 \qquad (3.12)$$

$$W \frac{d}{d\theta}(\psi_a - \psi_b) = 0 \qquad (3.13)$$

Substituting for ψ_a and ψ_b in above equation with $\beta = 60 - \alpha$ we get:

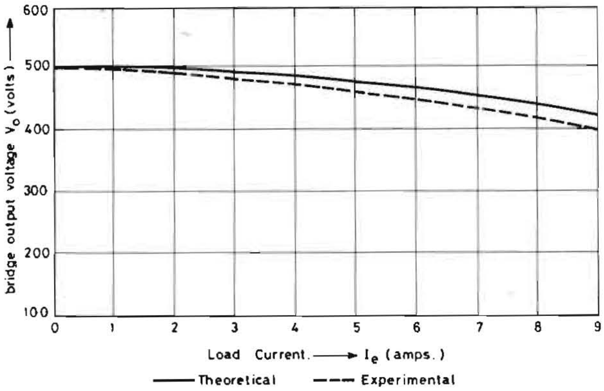

Fig. 4. Theoretical and experimental variation of bridge voltage with load current of a synchronous generator with h-g damper windings connected to uncontrolled bridge rectifier load.

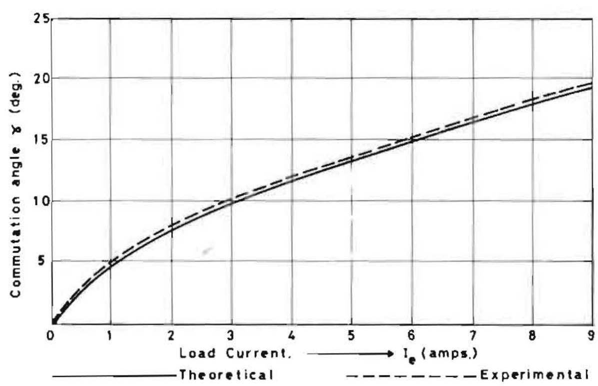

Fig. 5. Theoretical and experimental variation of communication angle with load current of a synchronous generator with h-g damper windings connected to uncontrolled bridge rectifier load.

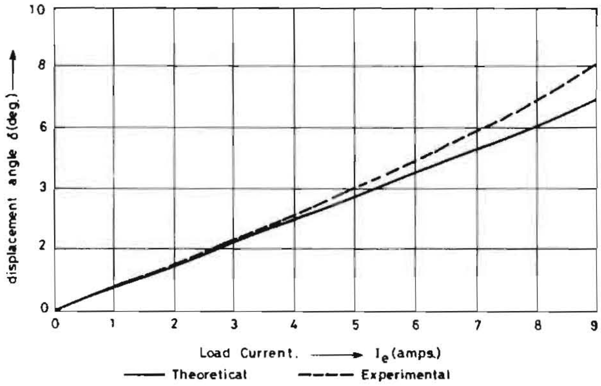

Fig. 6. Theoretical and experimental and variation of displacement angle with load current of a synchronous generator with h-g damper windings connected to uncontrolled bridge rectifier load.

$$0 = 2\sqrt{3}\, W L_{sv} I_e \sin 2(\delta + 60) + [W L_f (i_f)_1 + W L_h (i_h)_1 + L_g (p\, i_g)_1 \sin(\delta) - [L_f (p\, i_f)_1 + L_h (p\, i_h)_1 - W L_g (i_g)_1] \cos(\delta) \qquad (3.14)$$

Where $(i_f)_1$, $(i_h)_1$ and $(i_g)_1$ are the field and damper currents at $\beta = 60 - \alpha$. Also $(p\, i_f)_1$, $(p\, i_h)_1$, and $(p\, i_g)_1$ are the rate of change of field and damper currents at $\beta = 60 - \alpha$.

Substituting in equation (3.14) for $(i_f)_1$, $(i_h)_1$, $(i_g)_1$, $(p\, i_f)_1$, $(p\, i_h)_1$ and $(p\, i_g)_1$ we get;

$$[L_d - L_q]\, I_e \sin 2(\delta + 60) = - I_e [L''_d - L_d][K_1 \sin^2(\delta) + K_2 \sin(2\delta)] + I_e [L - L'']A + (\sqrt{3}/2)\, I_e [L_d - L''_d] - (\sqrt{3}/2)[L_f (i_f)_o + L_h (i_h)_o] \sin(\delta) - (\sqrt{3}/2)[L_g (i_g)_o] \cos(\delta) \qquad (3.15)$$

This equation illustrates the dependence of the displacement angle on the field and damper currents perturbation. For a load change the magnitude of δ will change accordingly.

3.5 The Average D.C. Output Voltage Equation

The average d. c. output voltage during the interlude interval can be written as follows:

$$V_e = \frac{\sqrt{3}\, 3W}{2} \left[\frac{I_e}{\sqrt{3}} (L_d - L_q) [\cos 2(\beta + \alpha + \gamma + 30) - \cos 2(\delta + \alpha - 30)] + [L_f (i_f) + L_h (i_h)] \cos(\delta + \alpha + \gamma) - [L_g (i_g)] \sin(\delta + \alpha + \gamma) + [L_f (i_f)_o + L_h (i_h)_o] \cos(\delta + \alpha) - [L_g (i_g)_o \sin(\delta + \alpha)] \right] \qquad (3.16)$$

Note that the second harmonic term is due to saliency.

The theoretical and practical performance of a laboratory generator with a bridge rectifier load compares favourably as shown in Figures 4 to 11.

Oscillograms of the transients during operation with the load variation at different controlled delay angles, for AC phase voltage, field current, and DC output voltages were recorded as shown in Figures 12 and 13 respectively.

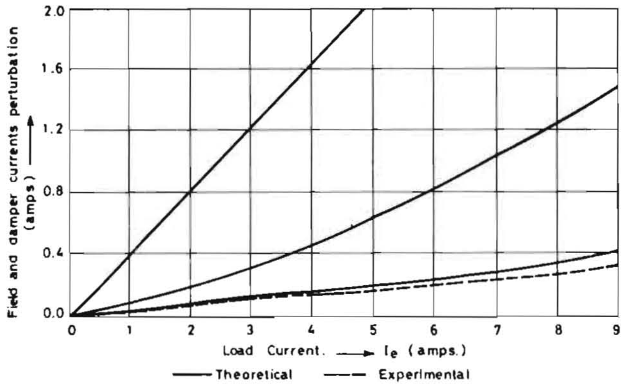

Fig. 7. Theoretical and experimental variation of field and damper current perturbation with load current of a synchronous generator with h-g damper windigs connected to uncontrolled bridge rectifier load.

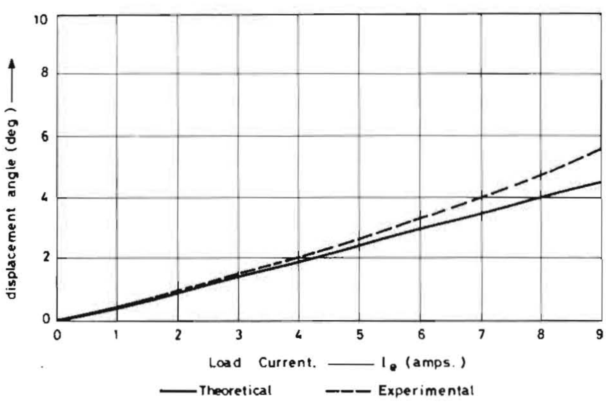

Fig. 8. Theoretical and experimental variation of displacement angle with load current of a synchronous generator with h-g damper windings connected to a thyristor bridge rectifier load at controlled delay angle = 20°.

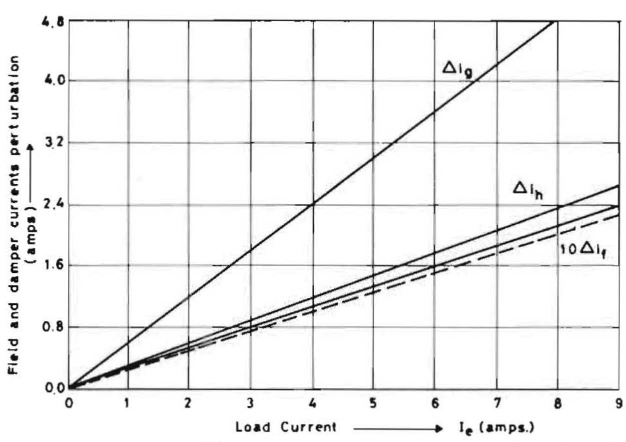

Fig. 9. Theoretical and experimental variation of field and damper current perturbation with load current at control delay angle equal 40°.

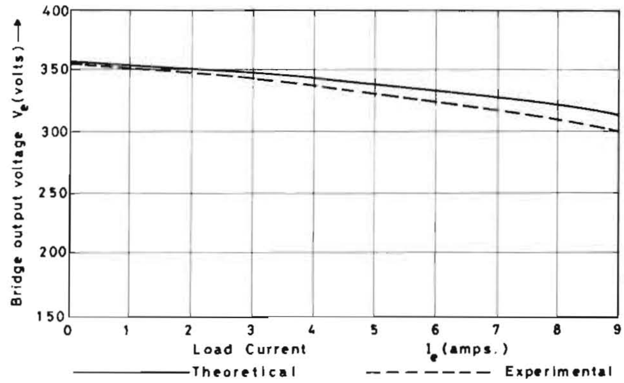

Fig. 10. Theoretical and experimental variation of bridge voltage with load current of a synchronous generator with h-g damper windings connected to a thyristor bridge load at control delay angle = 40°.

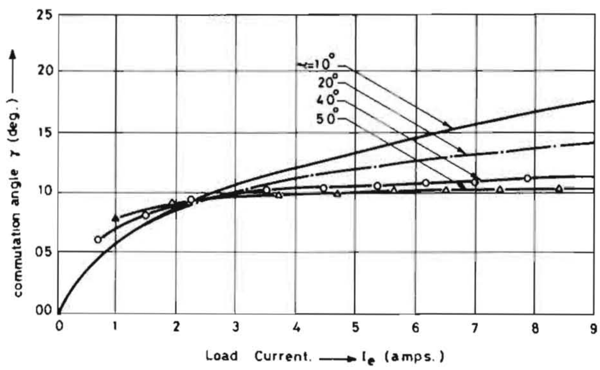

Fig. 11. Experimental variation of commutation angle with load current of a synchronous generator with h-g damper windings connected to a thyristor bridge rectifier, with different delay angles.

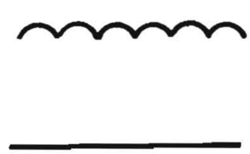

Fig. (12.a)
$\alpha = 0^{\circ}$
$I_f = 1.5$ A, $I_e = 1$ A

Fig. (12. b)
$\alpha = 0^{\circ}$
$I_f = 1.5$ A, I = 2 A

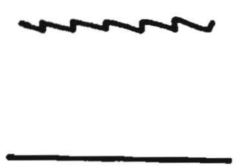

Fig.(13. a)
$\alpha = 20°$
$I_f = 1.5$ A, $I_e = 2$ A

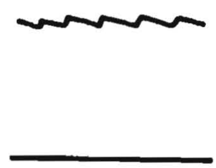

Fig.(13. b)
$\alpha = 20°$
$I_f = 1.5$ A, $I_e = 3$ A

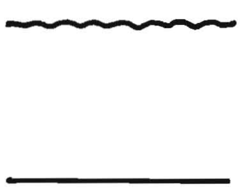

Fig.(13. c)
$\alpha = 20°$
$I_f = 1.5$ A, $I_e = 6$ A

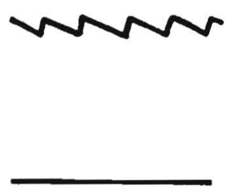

Fig.(13. d)
$\alpha = 40°$
$I_f = 1.5$ A, $I_e = 2$ A

4. Conclusions

This paper leads to the derivation of the basic equations for a star connected three – phase salient pole type synchronous generator loaded by a three phase HVDC system. Both saliency and asymmetrical damper windings are considered. Special cases, such as turbo–type generator, absence of damper windings, and or uncontrolled bridge loads, can be accommodated. Equations for the displacement angle, the commutation current, and the commutation angle, together with equations for the field and damper currents during the commutation and interlude intervals, field and damper currents perturbation, bridge voltage, and output power, allow the performance of the generator to be computed. In the present form, the solution of the basic set of equations requires an iteration process using a sufficiently accurate equation derived for $(i_f)_o$, $(i_h)_o$, $(i_g)_o$, $(i_f)_\gamma$, and $(i_g)_\gamma$. A special case for uncontrolled bridge loads, is also computed during the iteration process. It will be noted that the waveform distortion is observed to be most severe when the transient saliency is greatest. From the performance equations, a reduction in L''_d and L''_q would reduce the commutation angle and reduce the relative influence of the filed in the direct–axis, and leads to a decrease in subtransient saliency. It is concluded that:

- reducing the field and damper current perturbation to lower the generator losses becomes necessary,
- reducing the overlap as well as $(L_d - L_q)$ would reduce the overlap angle, but the generator voltage will contain less deformation due to less commutation angle,
- the control region will be limited by the maximum displacement angle associated with maximum loading of that case.

Appendix – A

$$K_f = \frac{L_f L_{hh} - L_h L_{hf}}{L_{ff} - L^2_{hf}} \qquad K_g = \frac{L_g}{L_{gg}}$$

$$K_h = \frac{L_h L_{ff} - L_f L_{hf}}{L_{ff} L_{hh} - L^2_{hf}} \qquad K_1 = A - \frac{3}{2}$$

$K_2 = (B - .35)$ $\quad A = (\sqrt{3}/2) + \cos(\alpha + 30)$

$B = [.5 \sin(\alpha + 30) - .25]$ $\quad L''_d = L_d - (3/2)[L_f K_f + L_h K_h]$

$L''_q = L_d - 3/2\,[L_g K_g]$

Appendix – B

The integral functions W and H can be obtained from the following:

$$W = \frac{(\pi/3) I_e}{(\pi/3) -} [\cos(\delta + \alpha + 30) - \cos(\delta + \alpha + \gamma - 30)]$$

$$+ I_e \sin(\delta + \alpha + \gamma)$$

$$H = \frac{-(\pi/3) I_e}{(\pi/3) - \gamma} [\sin(\delta + \alpha + 30) - \sin(\delta + \alpha + \gamma - 30)]$$

$$+ I_e \cos(\delta + \alpha + \gamma)$$

References

1. **Gerecke, E.**, «Synchronmaschine mit Stromrichterbelastung», *Neue Tech.* pp. 758–766 (1961).
2. **Garrido, M.S.**, «Theoretical and experimental study of the generator-rectifier: 1–Equations of the generator rectifier in steady state condition». *Rev. Ee(Belgium)* **7**, (3), pp. 60–71 (1972).
3. **Bugenstein, W.A.** «Transient behaviour of a.c. alternator with rectifier output», Proceedings of National Aerospace Electronics Conference, Dayton, Ohio, U.S.A., 19–21 May, 1969, (New York, U.S.A: IEEE 1968), pp. 233–236.
4. **Franklin, P.W.**, «A theoretical study of three phase salient pole type generator with simultaneous AC and bridge rectifier output (Part I and II)», *IEE. Trans. Power App. and System.* (U.S.A), Vol. **PAS. 92,** (2), PP. 543–57 (1973).
5. **Bonwick, W.J.**, «Synchronous generator with unbalanced bridge rectifier loads», Ins. Eng. Aust. Elec. Eng. Trans. (Australia) Vol. **EE10,** (1), PP. 39–45 (1974).

أداء المحركات التزامنية في شبكات الجهد الفائق وتأثيرها ببروز الاقطاب والتوحيد المحكوم وغير المحكوم

المرحوم محمد عباس شيمي منصور*، عبد العزيز السليمان**، س عبد الرازق***

* استاذ سابق - بقسم الهندسة الكهربائية - كلية الهندسة - جامعة الرياض.

** أستاذ مساعد - قسم الهندسة الكهربائية - كلبة الهندسة - جامعة الرياض.

*** كلية الهندسة - جامعة القاهرة - جمهورية مصر العربية.

في هذه المقالة يقدم الباحثون استنتاجا لخواص المحركات التزامنية تجريبيا ونظريا حين تعمل في شبكات الجهد الفائق مع الوضع في الاعتبار بروز الاقطاب والتوحيد (سواء كان محكوما أو حرا). وقد قدمت معادلات الأداء للنظام ككل مع الاخذ في الاعتبار بوجود ملفات إخماد أو عدم وجودها وكذلك يمكن تطويع هذه المعالجة للتعامل مع بعض الحالات الخاصة مثل المحركات التي تعمل بالتربينات، ولاثبات فعالية الطريقة فقد قورنت النتائج المعملية والنظرية.